Parasitology Research (2019) 118:2295–2304
https://doi.org/10.1007/s00436-019-06329-3

TREATMENT AND PROPHYLAXIS - ORIGINAL PAPER

Oleic acid–conjugated silver nanoparticles as efficient antiamoebic agent against *Acanthamoeba castellanii*

Ayaz Anwar[1] · Sumayah Abdelnasir Osman Abdalla[1] · Zara Aslam[2] · Muhammad Raza Shah[2] · Ruqaiyyah Siddiqui[1] · Naveed Ahmed Khan[1]

Received: 11 March 2019 / Accepted: 16 April 2019 / Published online: 15 May 2019

Abstract

Acanthamoeba castellanii belonging to the T4 genotype is an opportunistic pathogen which is associated with blinding eye keratitis and rare but fatal central nervous system infection. *A. castellanii* pose serious challenges in antimicrobial chemotherapy due to its ability to convert into resistant, hardy shell-protected cyst form that leads to infection recurrence. The fatty acid composition of *A. castellanii* trophozoites is known to be most abundant in oleic acid which chemically is an unsaturated *cis*-9-Octadecanoic acid and naturally found in animal and vegetable fats and oils. This study was designed to evaluate antiacanthamoebic effects of oleic acid against trophozoites, cysts as well as parasite-mediated host cell cytotoxicity. Moreover, oleic acid–conjugated silver nanoparticles (AgNPs) were also synthesized and tested against *A. castellanii*. Oleic acid–AgNPs were synthesized by chemical reduction method and characterized by ultraviolet-visible spectrophotometry, atomic force microscopy, dynamic light scattering analysis, and Fourier transform infrared spectroscopy. Viability, growth inhibition, encystation, and excystation assays were performed with 10 and 5 μM concentration of oleic acid alone and oleic acid–conjugated AgNPs. Bioassays revealed that oleic acid alone and oleic acid–conjugated AgNPs exhibited significant antiamoebic properties, whereas nanoparticle conjugation further enhanced the efficacy of oleic acid. Phenotype differentiation assays also showed significant inhibition of encystation and excystation at 5 μM. Furthermore, oleic acid and oleic acid–conjugated AgNPs also inhibited amoebae-mediated host cell cytotoxicity as determined by lactate dehydrogenase release. These findings for the first time suggest that oleic acid–conjugated AgNPs exhibit antiacanthamoebic activity that hold potential for therapeutic applications against *A. castellanii*.

Keywords *Acanthamoeba* · Silver nanoparticles · Oleic acid · Cyst · Cytotoxicity

Introduction

Acanthamoeba spp. are ubiquitous in a variety of natural environments worldwide, having been extracted from the air, soil, natural water, bottled water, vegetables, swimming pools, and even medical institutions (Marciano-Cabral and Cabral 2003; Khan 2006). These free-living protist pathogens are the causative agent of the fatal granulomatous amoebic encephalitis (GAE) and the painful, blinding *Acanthamoeba* keratitis (AK). GAE is a rare but deadly disease with mortality rate of 95% (Kulsoom et al. 2014). *Acanthamoeba* spp. alternate between two different stages namely trophozoites and cysts during their life cycle (Siddiqui and Khan 2012). Adverse environmental conditions induce the encystation of trophozoites into double-walled cysts. In addition to changes in temperature, pH, osmolarity, food scarcity, etc., drugs can also elicit cellular differentiation into resistant cyst form. As a result, in treating infections, no single drug has been found effective (Lorenzo-Morales et al. 2015). Currently, treatment of *Acanthamoeba* infections includes a combination of chemotherapeutic agents including biguanides which hinder cell membrane function such as polyhexamethylene biguanide (PHMB) or chlorhexidine (CHX) and aromatic diamidines which inhibit the synthesis of DNA such as propamidine

Handling Editor: Julia Walochnik

✉ Ayaz Anwar
ayazanwarkk@yahoo.com

[1] Department of Biological Sciences, School of Science and Technology, Sunway University, 47500 Subang Jaya, Selangor, Malaysia

[2] HEJ Research Institute of Chemistry, International Center for Chemical and Biological Sciences, University of Karachi, Karachi 75270, Pakistan

isethionate (Polat et al. 2014). Unfortunately, these biguanides and diamidines are toxic to human cells and toxic keratopathy has been observed as a side effect of the combination of PHMB and CHX (Lorenzo-Morales et al. 2015). Ultimately, cysticidal therapeutic agents that can traverse the blood-brain barrier and have minimal toxicity to human cells are required to treat infections effectively and prevent infection recurrence.

cis-9-Octadecenoic acid, commonly known as oleic acid, is a fatty acid found naturally in different types of plant and animal lipids. The plasma membrane of *Acanthamoeba* is made up of 25% phospholipids, a feature of which is the abundance of fatty acyl residues (Palusinska-Szysz et al. 2014). Oleic acid was found to be amongst the most abundant fatty acid in every phospholipid class in *Acanthamoeba*, comprising 40 to 50% (Palusinska-Szysz et al. 2014). This profusion of oleic acid suggests its contribution to the metabolism and growth of *Acanthamoeba*. Recently, Wu et al. (2018) suggested that such fatty acids can interact with the lipid membranes of microbes and as a result derange the electron transport chain and oxidative phosphorylation. As a result of trophozoite variability studies, they described the effects of treatment with oleic acid inhibit *A. castellanii* growth by induction of apoptosis by eliciting autophagy in trophozoites. In another report, it was observed that unsaturated fatty acids, with oleic acid being amongst the most effective, are potent uncouplers and protonophores in *A. castellanii* mitochondria, inhibiting ATP synthesis (Swida et al. 2007). Oleic acid has also been used to target *Entamoeba histolytica* amongst other fatty acids, all of which were effective in killing amoeba to some degree (Manna et al. 2013).

In recent years, nanotechnology has earned the interest of a vast audience in biotechnology, engineering, and medicine (Wilczewska et al. 2012). New studies report an increase in drug bioavailability and efficacy when conjugated to nanoparticles due to the reduction in size (Zazo et al. 2016). Nanoparticles have also been used as potent therapeutic agents against *A. castellanii* (Anwar et al. 2018a, b; Aqeel et al. 2016). Nanoparticles coated with plant extracts (e.g., *Jatropha curcas*, *Jatropha gossypifolia*, and *Euphorbia milii* (Borase et al. 2013); and *Pterocaulon balansae* (Panatieri et al. 2017), and natural products such as tannic acid (Padzik et al. 2018), periglaucine A and betulinic acid (Mahboob et al. 2018), hesperidin, and naringin (Anwar et al. 2019a, b) have been found to be effective antiacanthamoebic agents. In this study, we test the antiacanthamoebic capacity of oleic acid–conjugated AgNPs against *A. castellanii* clinical isolate belonging to the T4 genotype. The OA-AgNPs were synthesized by one-phase reduction of silver nitrate in the presence of oleic acid using sodium borohydride, and utilized in antiamoebic, host cell cytopathogenicity, cell cytotoxicity as well as encystation and excystation assays. Considering the challenges in developing new drugs, it is hoped that the use of commonly found naturally occurring fatty acid, i.e., oleic acid, is a useful choice in targeting infections caused by *A. castellanii*.

Materials and methods

Chemicals

Oleic acid used to synthesize the nanoparticles was of analytical grade and purchased from Sigma-Aldrich. Silver nitrate and sodium borohydride used in the synthesis of nanoparticles were purchased from Merck chemicals.

Synthesis of nanoparticles

Oleic acid was dissolved in 1 mL ethanol, and 50 mL volume was made up with deionized water to make a stock solution of 5 mM. Oleic acid–conjugated silver nanoparticles were synthesized by the reduction of silver nitrate solution using sodium borohydride in the presence of oleic acid as described previously (Anwar et al. 2016). One milliliter of 1 mM silver nitrate solution was magnetically stirred with 1 mL of 1 mM oleic acid before 5 μL of freshly prepared 5 mM sodium borohydride was added and stirring was continued for 2 h. The formation of oleic acid–conjugated AgNPs was identified by a color change from colorless to yellow brown indicative of reduction of silver ions. The same technique was used in the preparation of unconjugated AgNPs, which were newly prepared with every use due to their instability. Characterization of the nanoparticles was carried out by using ultraviolet-visible spectrophotometry (Evolution 300, Thermo Scientific), atomic force microscopy (Agilent 5500), dynamic light scattering analysis (Malvern instrument, UK), and Fourier transform infrared spectroscopy (Vector 22, Bruker).

Cultures of *A. castellanii*

A. castellanii (ATCC 50492) is a clinical isolate of the T4 genotype and was cultured in 10 mL of PYG medium: 0.75% (*w*/*v*) proteose peptone, 0.75% (*w*/*v*) yeast extract, and 1.5% (*w*/*v*) glucose in 75-cm^2 tissue culture flasks at 30 °C (Sissons et al. 2006). For use in assays, active adherent trophozoites were obtained by discarding old PYG containing dormant or dead cells, replacing it with RPMI-1640 and placing the flask on ice for 15 min before detaching with gentle tapping. The suspension was centrifuged for 10 min at 3000×*g* and the obtained pellet was resuspended in 1 mL of RPMI-1640 before enumerating cells using a hemocytometer.

Acanthamoeba viability assays

Antiamoebic assays were carried out as presented previously (Siddiqui et al. 2017). The effects of oleic acid (OA) alone,

silver nanoparticles (AgNPs) alone, and oleic acid–conjugated AgNPs (OA-AgNPs) was determined on the viability of amoebae. 5×10^5 *A. castellanii* trophozoites were treated with 5 μM and 10 μM of OA, AgNPs, and OA-AgNPs in RPMI-1640 in 24-well plates. 10 μM of chlorhexidine was used as a positive control in the assay and RPMI-1640 alone as a negative control. Plates were incubated for 24 h at 30 °C after which the viability of cells was determined by Trypan blue exclusion assay. Trypan blue (0.1 %) was added to each well and cells that were unstained (viable) were counted using a hemocytometer.

Amoebistatic assays

Amoebistatic assays were performed to determine the potential of the test samples in inhibiting the growth of *A. castellanii* (Sissons et al. 2006). 5 and 10 μM OA, AgNPs, and OA-AgNPs were tested against 5×10^5 trophozoites using growth medium (PYG). PYG medium alone was used as a negative control and 10 μM chlorhexidine was used as a positive control. Following the 24-h incubation time at 30 °C, Trypan blue (0.1 %) staining was used to enumerate the effects on amoebae growth.

Encystation assays

Encystation assays were performed as previously described (Siddiqui et al. 2017). 5×10^5 trophozoites were incubated in a 24-well plate with 5 μM and 10 μM OA, AgNPs, and OA-AgNPs in PBS containing an encystation medium comprised of 5 mM $MgCl_2$ and 8% glucose. The plate was incubated at 30 °C for 72 h, following which, 0.25% sodium dodecyl sulfate (SDS) was added for a maximum of 5 min in order to solubilize trophozoites but not cysts. Finally, cysts were counted using a hemocytometer and a number of cysts were determined.

Excystation assays

A. castellanii cysts were prepared as described previously (Dudley et al. 2009). Briefly, 1×10^6 trophozoites were inoculated on non-nutrient agar plates followed by incubation at 30 °C for up to 14 days. Next, the cysts were harvested thoroughly washing and scraping with 5 ml of phosphate-buffered saline (PBS). Cyst suspension was centrifuged at 3000×*g* for 10 min to collect the cyst pellet. These cysts were then resuspended in PBS, enumerated using a hemocytometer, and used in excystation assays. The effects of OA-AuNPs on excystation were measured by inoculating 5×10^5 *A. castellanii* cysts in PYG medium after treatment with 10 or 5 μM OA alone and OA-AuNPs in 24-well plates. Plates were incubated at 30 °C and observed under an inverted microscope every 24 h for up to 72 h to detect the emergence of trophozoites, which were counted using a hemocytometer.

HeLa cell culture

HeLa cells were obtained from ATCC (CCL-2) and cultured in RPMI-1640 containing 10% fetal bovine serum, 1% (2 mM) L-glutamine, 1% penicillin-streptomycin, and 1% minimal essential media non-essential amino acid (MEM NEAA) as previously described (Rajendran et al. 2017). The cells were preserved at 37 °C in a CO_2 incubator with 95% humidity. After the removal of existing media, confluent flasks were trypsinized with 2 mL trypsin and inoculated into 96-well plates for use in cytotoxicity and cytopathogenicity assays once a uniform monolayer is ensured through microscopy

Host cell cytopathogenicity assays

Amoeba-mediated HeLa cell cytotoxicity was assessed in 96-well plates with HeLa monolayers (Anwar et al. 2018a). 5×10^5 *A. castellanii* trophozoites were treated with 5 μM and 10 μM of OA, AgNPs, and OA-AgNPs in 24-well plates with RPMI-1640 and incubated at 30 °C for 2 h. Amoebae in RPMI-1640 was used as a negative control and chlorhexidine was used as a positive control. Following the 2-h incubation, treated amoebae was centrifuged at 3000×*g* for 10 min to separate extracellular components and pellet was resuspended in 200 μL RPMI-1640 before addition to HeLa cell monolayers. The plates were incubated for 24 h at 37 °C in a 5% CO_2 incubator. A negative control was achieved by incubating HeLa cells with RPMI-1640 only and a positive control was 100% cell death obtained by treating HeLa cells with 1% Triton X-100. After the incubation, the supernatant of each well was collected and the release of lactate dehydrogenase enzyme (LDH) was measured as an absorbance reading at 490 nm using a cytotoxicity detection kit. LDH is an intracellular enzyme that is released when cells are damaged. The percentage of cytopathogenicity was calculated as: (sample absorbance-negative control absorbance)/(positive control absorbance-negative control absorbance) × 100.

Cell cytotoxicity assays

Cytotoxicity of OA alone, AgNPs alone, and OA-AgNPs towards human cells was tested in 96-well plates with HeLa monolayers (Ali et al. 2017). 5 and 10 μM of the test samples were added to HeLa cells in RPMI-1640. The plates were then incubated in a 37 °C, 5% CO_2 incubator for 24 h. HeLa cells in RPMI-1640 only were taken as negative controls and maximum cell death by 1% Triton X-100 was used as a positive control. Following the 24-h incubation time, cell death was calculated as LDH release which is measured as an

absorbance reading at 490 nm. The percentage of cytotoxicity was calculated as follows: (sample absorbance-negative control absorbance)/(positive control absorbance-negative control absorbance) × 100.

Statistical analysis

The data presented is representative of several experiments performed in duplicates and plotted as the mean ± standard error. Significant differences were determined using two sample *t* test and two-tailed distribution in comparing the average of two independent groups on Microsoft Excel sheet. A critical value of $P < 0.05$ is used for all evaluations. In graphical presentation, y-axis error bars are indicative of the standard error of the data.

Results

Characterization of OA-AgNPs

OA-AgNPs were successfully synthesized using one-phase reduction of silver nitrate as described in "Materials and methods." When subjected to UV-Vis spectrophotometry, OA alone showed maximum absorbance at around 240 nm, while OA-AgNPs demonstrated maximum absorbance (λ max) at 408 nm, indicating the successful formation of oleic acid–conjugated silver nanoparticles (Fig. 1a). The morphological analysis of OA-AgNPs was carried out by AFM. OA-AgNPs were found to be spherical, and polydispersity index (PDI) was measured by DLS which is found to be 0.214 (Fig. 2a). Figure 2b shows the zeta potential scan of OA-AgNPs, where the zeta potential is found to be − 32.7 mV. The size distribution of OA-AgNPs is quite narrow under the circumstances of using strong reducing agent sodium borohydride which suggests the high stabilization efficiency of OA for AgNPs. The high negative charge on the surface of OA-AgNPs corresponds to the presence of negatively charged carboxylate groups. FT-IR analysis of OA in comparison to OA-AgNPs (Fig. 3) also suggests the interaction of carboxylate ions with AgNPs as the OH peaks are diminished, and carbonyl peak is shifted to higher energy in the later.

Oleic acid–conjugated AgNPs exhibited enhanced antiamoebic properties

Viability assays were carried out to assess the antiacanthamoebic effect of OA-AgNPs (Fig. 4a). Numbers of trophozoites were maintained at 5×10^5 in the negative control comprising of amoeba in RPMI-1640 alone. 5×10^5 *A. castellanii* trophozoites were reduced to 8.1×10^4 when treated with 10 μM of chlorhexidine used as a positive control. Significant effects on viability were observed when amoeba was treated with OA-AgNPs ($P < 0.05$ using two-sample *t* test and two-tailed distribution). The viability of *A. castellanii* was significantly reduced after treatment with 5 μM OA-AgNPs when compared to OA alone ($P < 0.05$ using two-sample *t* test and two-tailed distribution) (Fig. 4a). However, OA alone exhibited significant antiamoebic effects only at 10 μM. Furthermore, at 10 μM OA-AgNPs, numbers of viable *A. castellanii* trophozoites were reduced to 9.3×10^4. On the other hand, AgNPs alone and solvent controls did not cause any significant effects on viability of *A. castellanii*.

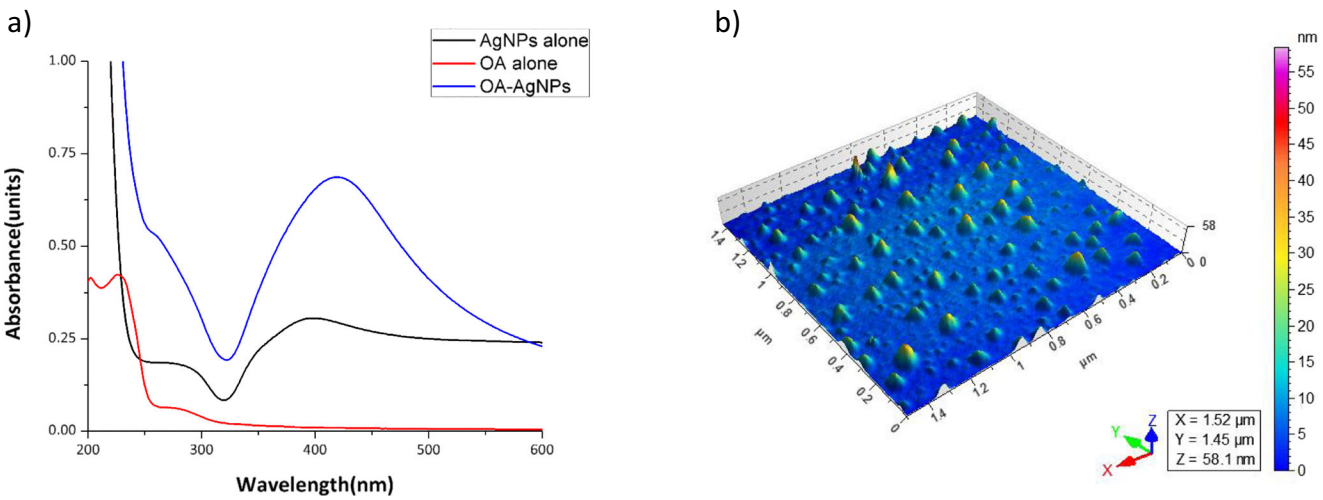

Fig. 1 **a** UV-Vis spectra of OA-AgNPs showing a characteristic surface plasmon resonance band at 408 nm confirming the formation of oleic acid–conjugated nanoparticles. UV-Vis spectra were recorded in aqueous phase and blank was corrected with deionized water. **b** Representative AFM image for morphological analysis of OA-AgNPs. OA-AgNPs were found to be spherical in shape with wide size distribution from 20 to 90 nm. Several images were recorded after casting a drop of OA-AgNPs on freshly cleaved mica surface followed by air drying, and AFM analysis was carried out in tapping mode by using SiN cantilever

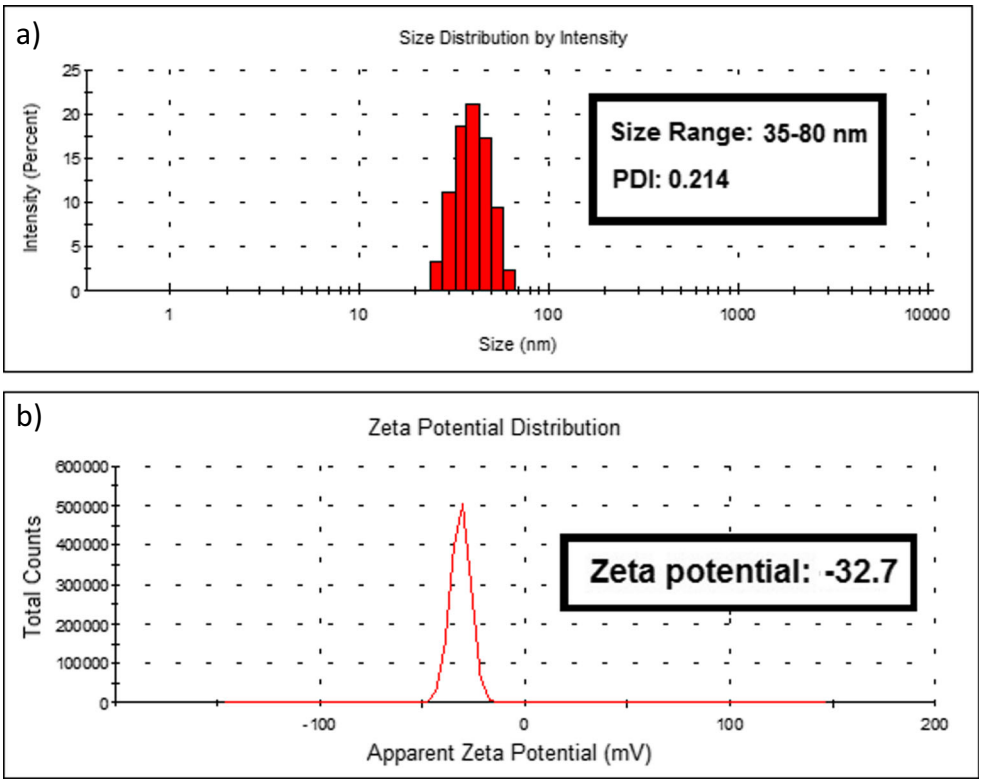

Fig. 2 **a** DLS zeta sizer scan of OA-AgNPs showing a relatively narrow size distribution in the range of 35–80 nm with the PDI 0.214. **b** Characteristic zeta potential of acid-conjugated AgNPs was observed at − 32.7 mV

Oleic acid–conjugated silver nanoparticles inhibited the growth of *A. castellanii*

The growth inhibition assay revealed that both OA alone and OA-AgNPs exhibited amoebistatic effects on the growth of *A. castellanii* (Fig. 4b). However, AgNP conjugation enhanced the growth inhibition of OA. In the negative control containing trophozoites in growth medium (PYG alone), the number of amoebae increased to 6.4×10^5 from the initial inoculum 5×10^5. Only 5.9×10^4 *A. castellanii* trophozoites were enumerated after treatment with 10 μM chlorhexidine which was used as a positive control. The growth of *A. castellanii* was significantly hindered upon treatment with OA-AgNPs ($P < 0.05$ using two-sample *t* test and two-tailed distribution) reducing numbers of viable amoeba to 1.2×10^5. The results of antiamoebic assays are also supported by representative images of each well recorded at × 200 magnification (Fig. 4c–h).

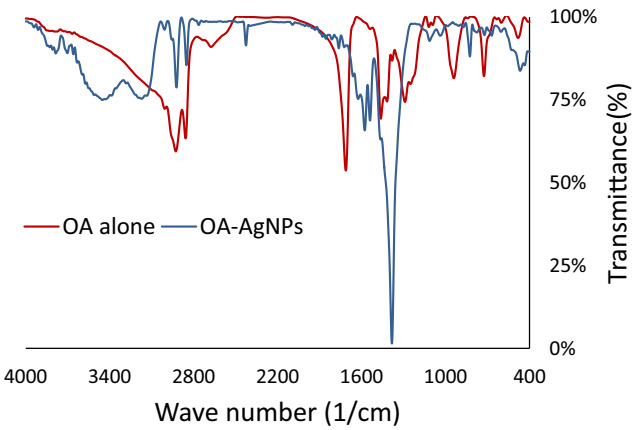

Fig. 3 Comparative FT-IR spectral analysis of OA alone with OA-AgNPs showing a characteristic alteration in the spectrum of OA when conjugated with AgNPs. The spectra were recorded by KBr disc method. Nanoparticles were freeze dried and mixed with analytical grade KBr to form a pellet which was analyzed by using FT-IR spectrometer (Vector 22, Bruker)

Oleic acid–conjugated silver nanoparticles inhibited encystation as well as excystation of *A. castellanii*

To discover the effects of OA-AgNPs on *A. castellanii*, encystation assays were performed. When 1×10^5 *A. castellanii* were incubated in the encystation medium, 3.8×10^4 cysts emerged after 72 h (Fig. 5a). Comparatively, this was significantly reduced after treatment with 10 μM OA-AgNPs where 8.7×10^3 cysts were enumerated, and 1.5×10^4 as compared to OA alone ($P < 0.005$ using two-sample *t* test and two-tailed distribution). However, a significant difference was not observed when OA-AgNPs were compared with OA alone at 5 μM. On the other hand, AgNPs alone and solvent controls did not inhibit encystation of *A. castellanii*.

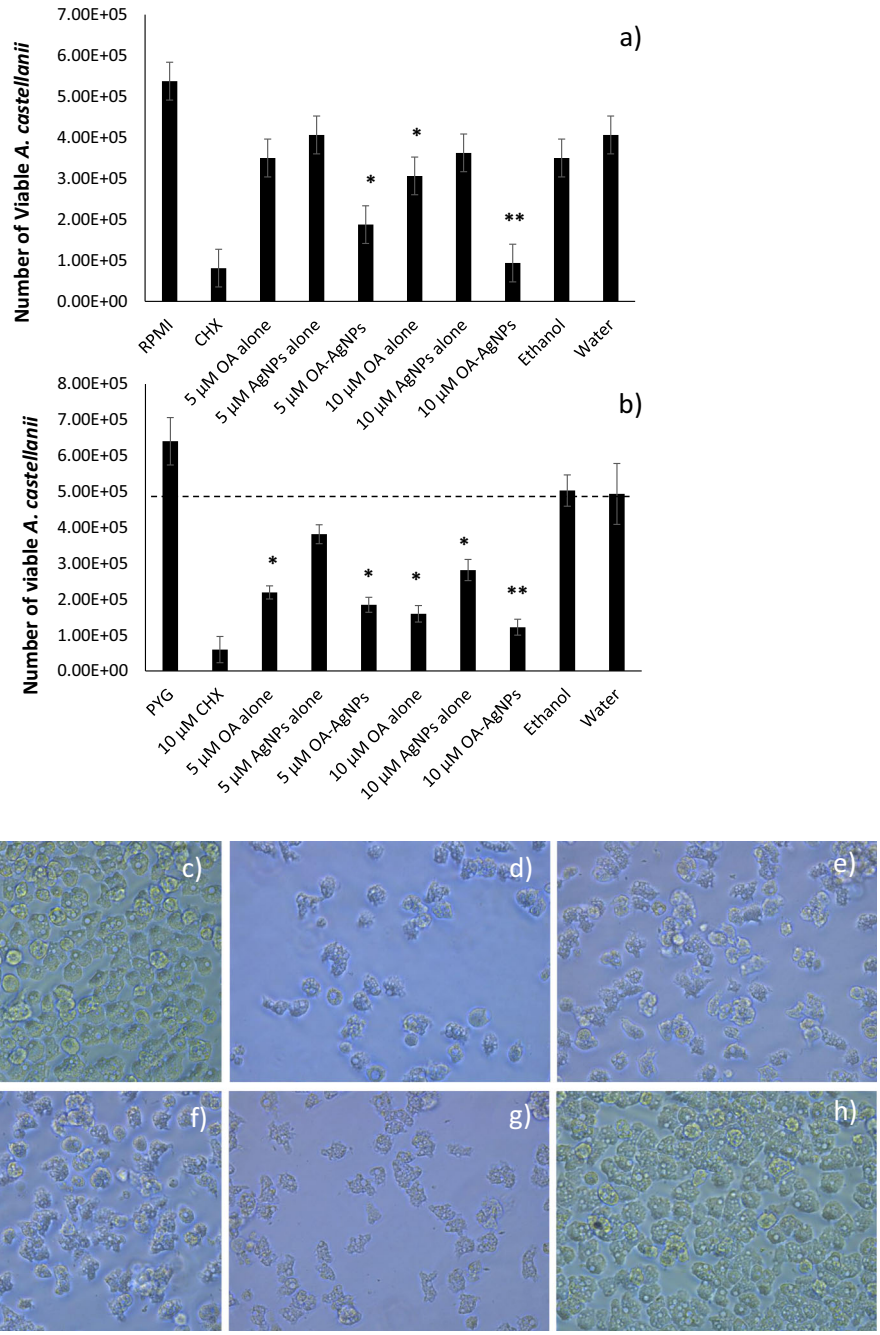

Fig. 4 **a** Antiamoebic effects of OA-AgNPs on *A. castellanii* belonging to the T4 genotype. In brief, 5×10^5 *A. castellanii* trophozoites were incubated with OA-AgNPs at 30 °C for 24 h after which viability was determined by staining with Trypan blue. The results show significant antiacanthamoebic activity when compared to the control (***$P < 0.001$, **$P < 0.005$, *$P < 0.05$ using two sample *t* test and two-tailed distribution). **b** Amoebistatic effects of OA-AgNPs on *A. castellanii* belonging to the T4 genotype. In brief, 5×10^5 *A. castellanii* trophozoites were incubated with OA-AgNPs at 30 °C for 24 h after which the growth was measured by enumeration of cells after staining with Trypan blue. The results show significant inhibition of growth when compared to the control (***$P < 0.001$, **$P < 0.005$, *$P < 0.05$ using two sample *t* test and two-tailed distribution). **c**–**h** Representative images of the antiamoebic assay. **c** Negative control. **d** Positive control. **e** OA alone at 10 μM. **f** AgNPs alone at 10 μM. **g** OA-AgNPs at 10 μM. **h** Solvent control

Interestingly, during excystation, only OA-AgNPs inhibited the process at both 10 and 5 μM where OA alone failed to exhibit any significant effects along with AgNPs alone and solvent controls (Fig. 5b). These results suggest the potential of AgNP conjugation with OA for enhanced antiamoebic effects.

Oleic acid–conjugated silver nanoparticles inhibited *A. castellanii*–mediated host cell cytopathogenicity

To assess possible inhibition of amoeba's pathogenicity to host cells, host cell cytopathogenicity assays were performed

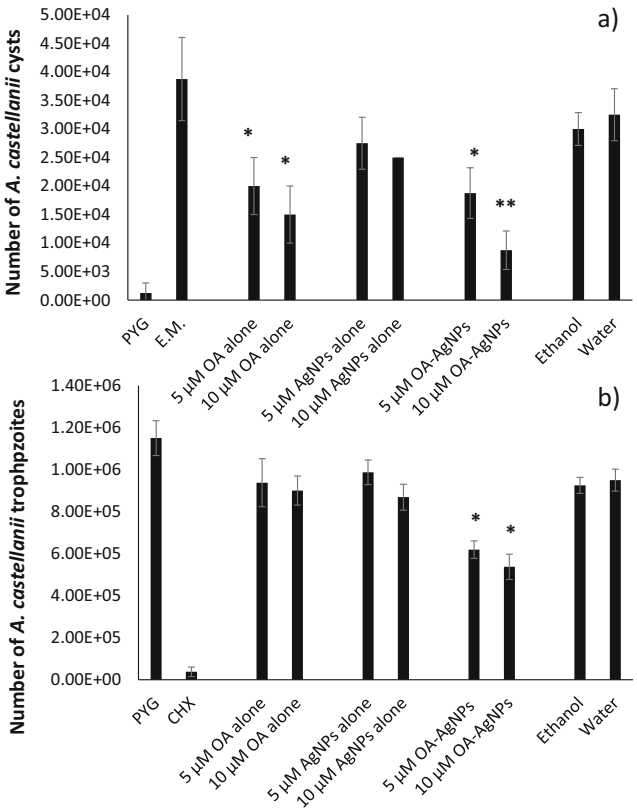

Fig. 5 **a** Effects of OA-AgNPs on the encystation of *A. castellanii* belonging to the T4 genotype. In brief, 5×10^5 *A. castellanii* trophozoites were incubated with an encystation media (8% glucose, 5 mM $MgCl_2$) and OA-AgNPs at 30 °C for 72 h. Subsequently, cysts were enumerated after treating with 0.25% SDS. The results show significant inhibition of encystation when compared to the control (***$P < 0.001$, **$P < 0.005$, *$P < 0.05$ using two sample *t* test and two-tailed distribution). **b** Excystation assay was performed to evaluate the dedifferentiation of *A. castellanii* from cysts into trophozoites. Briefly, 5×10^5 *A. castellanii* cysts were incubated with OA-AgNPs in growth medium (PYG) at 30 °C for 72 h. After incubation, cysts emerged into trophozoites were enumerated using hemocytometer. The results show significant inhibition of encystation when compared to the control (***$P < 0.001$, **$P < 0.005$, *$P < 0.05$ using two sample *t* test and two-tailed distribution)

as described in the "Materials and methods" section. Untreated *A. castellanii* produced 73% cytotoxicity to HeLa cells (Fig. 6a). On the contrary, pre-treatment with OA alone, AgNPs alone as well as OA-AgNPs notably reduced this pathogenicity at 10 μM. However, at 5 μM, none of the test samples significantly reduced the *A. castellanii*–mediated cytotoxicity except OA-AgNPs (Fig. 6a).

Cell cytotoxicity assays were carried out to determine the toxicity of OA-AgNPs against HeLa cells. 10 μM of chlorhexidine produced about 35% cytotoxicity to HeLa cells. Comparatively, none of the test samples exhibit more than 18% toxicity to HeLa cells (Fig. 6b). These results suggest that OA and OA-AgNPs may serve as safer alternatives against infections caused by *A. castellanii*.

Discussion

Despite progress in antimicrobial chemotherapy, infections due to *Acanthamoeba* spp. have remained substantial. As a result, there is a grave need for the development of therapy that effectively circumvents the drawbacks that current antiacanthamoebic drugs possess. These include chlorhexidine, amphotericin B, fluconazole, polyhexamethylene biguanide, or a mixture of these drugs which face obstacles in drug delivery due to their cytotoxic effects on human cells and tissues, limited blood-brain barrier penetration, and cellular differentiation of *Acanthamoeba* trophozoites into resistant cysts (Lorenzo-Morales et al. 2015). The pharmacodynamics and pharmacokinetics of drugs can be enhanced using nanomaterial-based drug delivery systems (Walsh et al. 2012) including liposomes and nanoparticles which have been utilized in clinical practice (Anselmo and Mitragotri 2016). These features manifest as an increased bioavailability and efficacy of drugs, decreased side effects, and effective lower dosages. Recently, silver nanoparticle drug conjugation was observed to enhance effects of amphotericin B and nystatin against *A. castellanii* as well as *N. fowleri* (Anwar et al. 2018a; Rajendran et al. 2017).

Fatty acids including oleic acid play vital biological roles, have important contributions in signal transduction pathways, and are essential in sustenance. Fatty acids have been seen to retain antimicrobial characteristics towards some bacteria and protists (Desbois and Smith 2010). Although the mechanism by which fatty acids kill or inhibit the growth of these microbes is unclear, it has been suggested that interaction with lipid membranes and subsequent disruption of the electron transport chain is a possible explanation (Manna et al. 2013). Fatty acids including oleic acid were found to have amoebicidal effects against *Entamoeba histolytica* (Manna et al. 2013). Thereafter, oleic acid has been shown to induce apoptosis in *A. castellanii* by induction of autophagy (Wu et al. 2018). Other studies have shown that oleic acid is an active uncoupler and protonophore in *A. castellanii* (Swida et al. 2007). These findings suggest potential in the use of oleic acid as an antimicrobial agent against *Acanthamoeba*. Here, we discovered the antiacanthamoebic effects of oleic acid–conjugated silver nanoparticles (OA-AgNPs) on *A. castellanii* belonging to the T4 genotype. OA-AgNPs were successfully synthesized, and when subjected to UV-Vis spectrophotometry, a characteristic surface plasmon resonance band was achieved at 408 nm. Viability assay results revealed that oleic acid–conjugated AgNPs exhibited antiacanthamoebic effects more effectively than oleic acid alone at both 5 and 10 μM concentrations. Notably, 10 μM OA-AgNPs had similar antiamoebic effects to 10 μM chlorhexidine. Amoebistatic results supported findings of viability assays and revealed marked hindrance of *A. castellanii* growth under advantageous conditions. As a secondary screening to

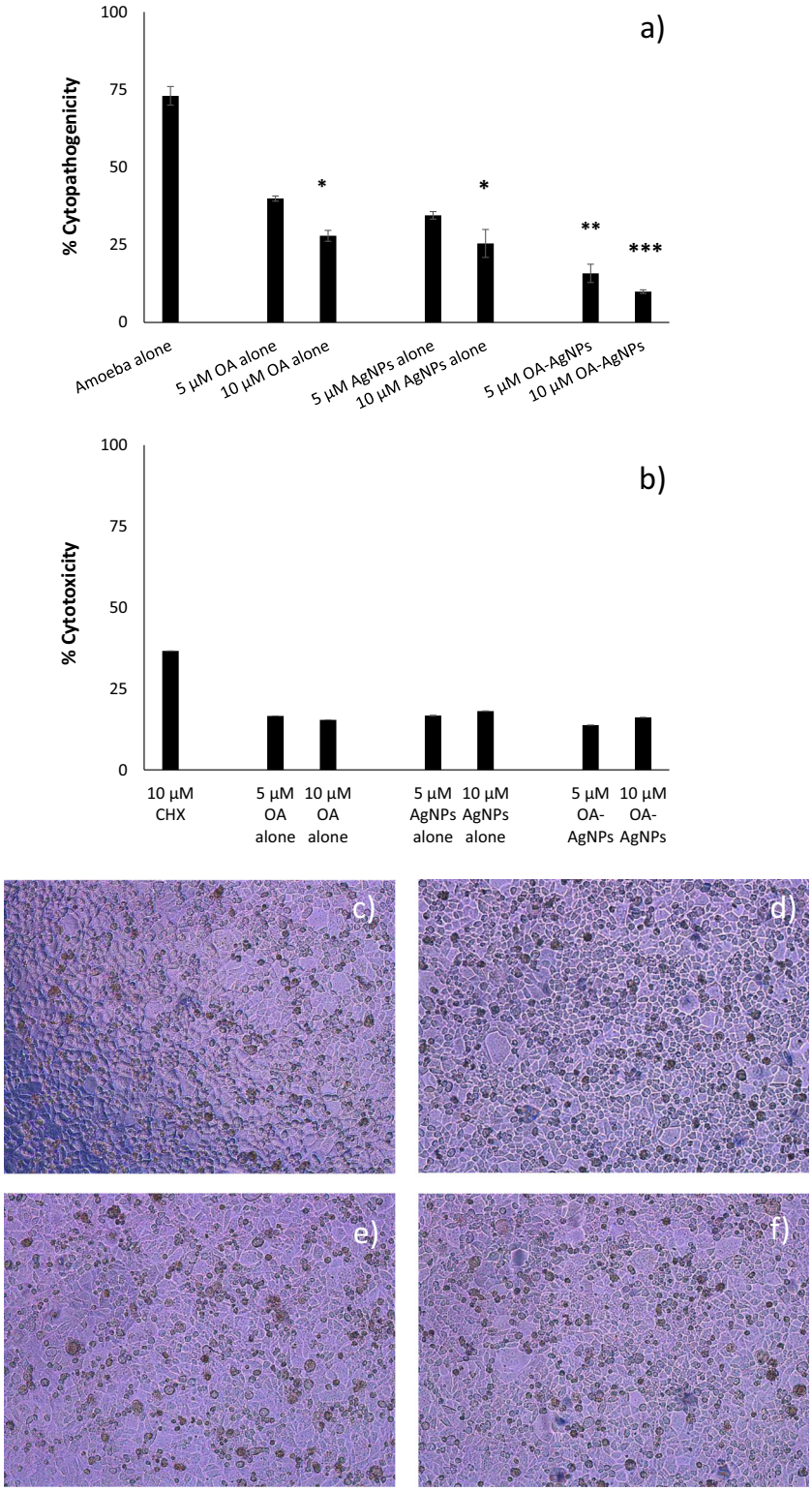

Fig. 6 **a** Pre-treatment of amoeba with OA-AgNPs inhibited HeLa cell cytopathogenicity. In brief, 5×10^5 *A. castellanii* trophozoites were incubated with OA-AgNPs at 30 °C for 2 h. Treated amoeba was then added to HeLa cells and incubated for 24 h at 37 °C in a 5% CO_2 incubator. The results show significant inhibition of cytopathogenicity when compared to untreated amoeba (***$P < 0.001$, **$P < 0.005$, *$P < 0.05$ using two sample *t* test and two-tailed distribution). **b** OA alone and OA-AgNPs presented limited cytotoxicity to HeLa cells. Briefly, 5 μM and 10 μM of OA, AgNPs, and OA-AgNPs were added to HeLa cells and incubated for 24 h at 37 °C in a 5% CO_2 incubator. The results show significantly lower cytotoxicity when compared to 10 μM of the antiamoebic drug chlorhexidine (CHX) (***$P < 0.001$, **$P < 0.005$, *$P < 0.05$ using two sample *t* test and two-tailed distribution). **c**–**f** Representative images of the cytotoxicity assay. **c** Negative control. **d** OA alone at 10 μM. **e** AgNPs alone at 10 μM. **f** OA-AgNPs at 10 μM

the effects of OA-AgNPs, host cell cytopathogenicity assays were conducted. Untreated *A. castellanii* produced 70% cytopathogenicity to HeLa cells while treatment with oleic acid and OA-AgNPs reduced this cytopathogenicity significantly producing about 11% and 6% cytopathogenicity respectively. Moreover, OA-AgNPs were also tested for cytotoxicity against HeLa cells by LDH cytotoxicity assays. When compared to the toxicity of CHX, an antiacanthamoebic drug that is currently in clinical practice, OA-AgNPs was 50% less cytotoxic at the same concentration. 10 μM of CHX produced 35% cytotoxicity to host cells, whereas 10 μM OA-AgNPs was 17% cytotoxic. This suggests potential for the use of OA-AgNPs as safer alternative. Nevertheless, more relevant cell lines including brain endothelial cells and corneal epithelium cells should be used in cytotoxicity and cytopathogenicity assays in the future before any in vivo studies are performed and that will be the subject of future studies.

These results are consistent with our previous findings where conjugation with AgNPs enhanced the antiamoebic properties of drugs (Anwar et al. 2019a, b). This is possibly due to the enhanced transport of oleic acid due to increased surface area and reduced size of the nanoparticles in comparison to oleic acid alone. AgNPs have been previously observed to retain antimicrobial properties against bacteria as well as protists (Golinska et al. 2014). Albeit their modes of action are not fully understood, their potency has been found to adjust with changes in its shape, size, and surface properties. Their interaction with microbial walls, penetration into the cells, formation of reactive oxygen species, and free radicals are also believed to be associated with their inhibitory effects (Dakal et al. 2016). Furthermore, the inhibition of encystation is a favorable feature for development of antiacanthamoebic agents, as when cellular differentiation into resistant cysts is blocked, the chances of amoeba surviving chemotherapeutic agents are diminished. Failure in the treatment of *Acanthamoeba* infections is largely due to the recurrence of infections due to cysts that have survived treatment (Siddiqui et al. 2016). Therefore, the inhibition of excystation by OA-AgNPs is a positive finding and higher concentrations of OA-AgNPs should be assessed for effects as they appear to be dose dependent.

In conclusion, these findings presented potential in the use of OA-AgNPs against *Acanthamoeba* due to their antiamoebic and amoebistatic effects as well as inhibition of encystation and excystation. Conjugation to AgNPs enhanced the effects of OA-AgNPs on the viability of amoeba believed to be due to the effective transport of oleic acid to the pathogen. Owing to the limited options in the treatment of these infections, it is hoped that silver nanoparticles conjugated to fatty acids including oleic acid could be a new promising avenue to discover. The blood-brain barrier penetration capacity of the nanoparticles may also be determined using in vitro blood-brain barrier models. Additionally, in vivo studies taking into consideration administration routes to assess potential in biological systems as opposed to cells in isolation will be carried out in future studies to determine translational value of these findings.

Acknowledgements This work is supported by University Research Award, Sunway University, Malaysia.

Funding This work was supported by the university's internal funding.

References

Ali SM, Siddiqui R, Ong SK, Shah MR, Anwar A, Heard PJ, Khan NA (2017) Identification and characterization of antibacterial compound (s) of cockroaches (*Periplaneta americana*). Appl Microbiol Biotechnol 101:253–286

Anselmo A, Mitragotri S (2016) Nanoparticles in the clinic. Bioeng Transl Med 1:10–29

Anwar A, Masri A, Rao K, Rajendran K, Khan NA, Shah MR, Siddiqui R (2019a) Antimicrobial activities of green synthesized gums-stabilized nanoparticles loaded with flavonoids. Sci Rep 9(1):3122

Anwar A, Rajendran K, Siddiqui R, Shah MR, Khan NA (2019b) Clinically approved drugs against CNS diseases as potential therapeutic agents to target brain-eating amoebae. ACS Chem Neurosci 10:658–666

Anwar A, Shah MR, Muhammad SP, Afridi S, Ali K (2016) Thiopyridinium capped silver nanoparticle based supramolecular recognition of Cu (I) in real samples and T-lymphocytes. New J Chem 40: 6480–6486

Anwar A, Siddiqui R, Hussain MA, Ahmed D, Shah MR, Khan NA (2018a) Silver nanoparticle conjugation affects antiacanthamoebic activities of amphotericin B, nystatin, and fluconazole. Parasitol Res 117:265–271

Anwar A, Siddiqui R, Shah MR, Khan NA (2018b) Gold nanoparticle conjugated Cinnamic acid exhibit antiacanthamoebic and antibacterial properties. Antimicrob Agents Chemother 62:e00630-18

Aqeel Y, Siddiqui R, Anwar A, Shah MR, Khan NA (2016) Gold nanoparticle conjugation enhances the antiacanthamoebic effects of chlorhexidine. Antimicrob Agents Chemother 60:1283–1288

Borase HP, Patil CD, Sauter IP, Rott MB, Patil SV (2013) Amoebicidal activity of phytosynthesized silver nanoparticles and their in vitro cytotoxicity to human cells. FEMS Microbiol Lett 345:127–131

Dakal TC, Kumar A, Majumdar RS, Yadav V (2016) Mechanistic basis of antimicrobial actions of silver nanoparticles. Front Microbiol 7: 1831

Desbois AP, Smith VJ (2010) Antibacterial free fatty acids: activities, mechanisms of action and biotechnological potential. Appl Microbiol Biotechnol 85:1629–1642

Dudley R, Jarroll EL, Khan NA (2009) Carbohydrate analysis of *Acanthamoeba castellanii*. Exp Parasitol 122:338–343

Golinska P, Wypij M, Ingle AP, Gupta I, Dahm H, Rai M (2014) Biogenic synthesis of metal nanoparticles from actinomycetes: biomedical applications and cytotoxicity. Appl Microbiol Biotechnol 98: 8083–8097

Khan NA (2006) *Acanthamoeba*: biology and increasing importance in human health. FEMS Microbiol Rev 30:564–595

Kulsoom H, Baig AM, Siddiqui R, Khan NA (2014) Combined drug therapy in the management of granulomatous amoebic encephalitis due to *Acanthamoeba* spp., and *Balamuthia mandrillaris*. Exp Parasitol 145:115–120

Lorenzo-Morales J, Khan NA, Walochnik J (2015) An update on *Acanthamoeba* keratitis: diagnosis, pathogenesis and treatment. Parasite 2015:22

Mahboob T, Nawaz M, Tian-Chye T, Samudi C, Wiart C, Nissapatorn V (2018) Preparation of poly (dl-lactide-co-glycolide) nanoparticles encapsulated with periglaucine A and betulinic acid for in vitro anti-*Acanthamoeba* and cytotoxicity activities. Pathogens 7(3):62

Manna D, Grewal JS, Sarkar B, Maiti S, Lohia A (2013) Polyunsaturated fatty acids induce polarized submembranous F-actin aggregates and kill *Entamoeba histolytica*. Cytoskeleton 70:260–268

Marciano-Cabral F, Cabral G (2003) *Acanthamoeba* spp. as agents of disease in humans. Clin Microbiol Rev 16:273–307

Padzik M, Hendiger EB, Chomicz L, Grodzik M, Szmidt M, Grobelny J, Lorenzo-Morales J (2018) Tannic acid-modified silver nanoparticles as a novel therapeutic agent against *Acanthamoeba*. Parasitol Res 117:3519–3525

Palusinska-Szysz M, Kania M, Turska-Szewczuk A, Danikiewicz W, Russa R, Fuchs B (2014) Identification of unusual phospholipid fatty Acyl compositions of *Acanthamoeba castellanii*. PLoS One 9(7):e101243

Panatieri LF, Brazil NT, Faber K, Medeiros-Neves B, von Poser GL, Rott MB, Zorzi GK, Teixeira HF (2017) Nanoemulsions containing a coumarin-rich extract from *Pterocaulon balansae* (*Asteraceae*) for the treatment of ocular *Acanthamoeba* keratitis. AAPS PharmSciTech 18:721–728

Polat ZA, Walochnik J, Obwaller A, Vural A, Dursun A, Arici MK (2014) Miltefosine and polyhexamethylene biguanide: a new drug combination for the treatment of *Acanthamoeba* keratitis. Clin Exp Ophthalmol 42:151–158

Rajendran K, Anwar A, Khan NA, Siddiqui R (2017) Brain-eating amoebae: silver nanoparticle conjugation enhanced efficacy of anti-amoebic drugs against *Naegleria fowleri*. ACS Chem Neurosci 8: 2626–2630

Siddiqui R, Abjani F, Yeo CI, Tiekink ER, Khan NA (2017) The effects of phosphanegold (I) thiolates on the biological properties of *Acanthamoeba castellanii* belonging to the T4 genotype. J Negat Results Biomed 16(1):6

Siddiqui R, Aqeel Y, Khan NA (2016) The development of drugs against *Acanthamoeba* infections. Antimicrob Agents Chemother 60:6441-6450.

Siddiqui R, Khan NA (2012) Biology and pathogenesis of *Acanthamoeba*. Parasit Vectors 5(1):6

Sissons J, Alsam S, Stins M, Rivas AO, Morales JL, Faull J, Khan NA (2006) Use of *in vitro* assays to determine effects of human serum on biological characteristics of *Acanthamoeba castellanii*. J Clin Microbiol 44:2595–2600

Swida A, Czarna M, Woyda-Płoszczyca A, Kicinska A, Sluse FE, Jarmuszkiewicz W (2007) Fatty acid efficiency profile in uncoupling of *Acanthamoeba castellanii* mitochondria. J Bioenerg Biomembr 39:109–115

Walsh MD, Hanna SK, Sen J, Rawal S, Cabral CB, Yurkovetskiy AV, Fram RJ, Lowinger TB, Zamboni WC (2012) Pharmacokinetics and antitumor efficacy of XMT-1001, a novel, polymeric topoisomerase I inhibitor, in mice bearing HT-29 human colon carcinoma xenografts. Clin Cancer Res 18:2591–2602

Wilczewska AZ, Niemirowicz K, Markiewicz KH, Car H (2012) Nanoparticles as drug delivery systems. Pharmacol Rep 64:1020–1037

Wu D, Qiao K, Feng M, Fu Y, Cai J, Deng Y, Tachibana H, Cheng X (2018) Apoptosis of *Acanthamoeba castellanii* trophozoites induced by oleic acid. J Eukaryot Microbiol 65:191–199

Zazo H, Colino CI, Lanao JM (2016) Current applications of nanoparticles in infectious diseases. J Control Release 224:86–102